Geophysical Prospecting, 2002, **50**, 615–627

Wave velocities and attenuation of shaley sandstones as a function of pore pressure and partial saturation

Nam H. Pham,[1]† José M. Carcione,[2] Hans B. Helle[3]* and Bjørn Ursin[1]

[1]*Norwegian University of Science and Technology, Department of Petroleum Engineering and Applied Geophysics, 7491 Trondheim, Norway,* [2]*Istituto Nazionale di Oceanografia e di Geofisica Sperimentale, Borgo Grotta Gigante 42c, 34010 Sgonico, Trieste, Italy, and* [3]*Norsk Hydro a.s., E & P Research Centre, PO Box 7190, 5020 Bergen, Norway*

Received July 2001, revision accepted July 2002

ABSTRACT

We obtain the wave velocities and quality factors of clay-bearing sandstones as a function of pore pressure, frequency and partial saturation. The model is based on a Biot-type three-phase theory that considers the coexistence of two solids (sand grains and clay particles) and a fluid mixture. Additional attenuation is described with the constant-Q model and viscodynamic functions to model the high-frequency behaviour. We apply a uniform gas/fluid mixing law that satisfies the Wood and Voigt averages at low and high frequencies, respectively. Pressure effects are accounted for by using an effective stress law. By fitting a permeability model of the Kozeny–Carman type to core data, the model is able to predict wave velocity and attenuation from seismic to ultrasonic frequencies, including the effects of partial saturation. Testing of the model with laboratory data shows good agreement between predictions and measurements.

INTRODUCTION

Wave velocities and attenuation are two important properties which can give information about lithology, saturation and the *in situ* conditions of rocks. It is therefore important to obtain a relationship between these properties and clay content, porosity, pore and confining pressures, frequency and pore-fluid saturation.

Modelling of the acoustic properties of shaley sandstones was achieved by Carcione, Gurevich and Cavallini (2000) in the framework of Biot's theory of poroelasticity. Unlike previous theories, this approach uses a Biot-type three-phase theory that considers the coexistence of two solids (sand grains and clay particles) and a fluid. The theory is generalized here to include the effects of pore pressure, partial saturation and the presence of a different type of dissipation mechanism.

Pressure effects are introduced by using an effective stress law. As is well known, at constant effective pressure the acoustic (or transport) properties of the rock remain constant. The effective pressure depends on the difference between the confining and pore pressures, the latter multiplied by the effective stress coefficient. In general, this coefficient is not equal to 1 and, therefore, the Terzaghi effective pressure law (i.e. the differential pressure) is not an appropriate quantity to describe the acoustic properties of the rock and varying pore pressure. However, a proper determination of the effective stress coefficient requires measurements of wave velocity as a function of confining and pore pressure. As Zimmerman (1991, p. 43) shows, if the rock is composed of a linear elastic grain material and the properties do not depend on the length scale of the pore structure, the dry-rock effective stress coefficient is equal to 1.

The effect of partial saturation on velocity and attenuation depends on the frequency range. At low frequencies, the fluid has enough time to achieve pressure equilibration (relaxed regime). In this case, the Wood model for the bulk modulus of the fluid mixture yields results that agree with the experiments (Mavko and Mukerji 1998). On the other hand, at high frequencies the fluid cannot relax and this state of unrelaxation induces a stiffening of the pore material,

*E-mail: hans.b.helle@nho.hydro.com
†Present address: Statoil ASA, PO Box 273, 7501 Stjørdal, Norway.

which increases the wave velocity considerably (Cadoret, Marion and Zinszner 1995). This effect implies an uneven distribution of fluids in the pore space, which is normally termed patchy saturation. In this case, Wood's model is not appropriate and, in general, a Hill average is used to model the wave velocities at ultrasonic (laboratory) frequencies. No microstructural theory is able to predict the behaviour at intermediate frequencies. In the present model we use a modified empirical fluid mixing law proposed by Brie *et al.* (1995), which gives the Wood modulus at low frequencies and the Voigt modulus at high frequencies.

Attenuation is described by using a constant-Q model for the dry-rock moduli (Kjartansson 1979; Carcione *et al.* 2001a). This approach is phenomenological, since a theory describing all the attenuation mechanisms present in a real sandstone is difficult, if not impossible, to develop. The constant-Q kernel is the simplest model based on only one parameter. We assume that the lower the frame modulus, the lower the quality factor (i.e. the higher the attenuation). Using this property, we assign a Q factor to the sandstone bulk modulus, and obtain the Q factor associated with the shear modulus. The Biot attenuation mechanisms are modelled by the original theory (Carcione *et al.* 2000), and, here, we introduce high-frequency viscodynamic effects, based on an optimal viscodynamic function obtained by Johnson, Koplik and Dashen (1987).

Pointer, Liu and Hudson (2000) described three distinct mechanisms of wave-induced fluid flow (see also Hudson, Liu and Crampin 1996): flow between cracks, flow within cracks and diffusion from cracks to the background porous medium. These mechanisms can be incorporated into the present theory by using Zener models of attenuation. The effects of partial saturation were investigated, for instance, by Hudson (1988). Under compression, the liquid is driven into the space previously occupied by gas. This movement is of a local fluid-flow nature and introduces a relaxation peak of the Zener type – or Maxwellian type, according to Pointer *et al.* (2000). Local fluid flow is modelled in the present theory by using a Zener element (e.g. Carcione 2001b, p. 65).

The sand/clay acoustic model for shaley sandstones, developed by Carcione *et al.* (2000), yields the seismic velocities as a function of clay (shale) content, porosity, saturation, dry-rock moduli, and fluid and solid-grain properties. As stated in previous work (Carcione and Gangi 2000a, b), the large change in seismic velocity is mainly due to the fact that the dry-rock moduli are sensitive functions of the effective pressure, with the largest changes occurring at low differential pressures. The major effect of porosity changes is implicit in the dry-rock moduli. Explicit changes in porosity and saturation are important but have less influence than changes in the moduli. In this sense, porosity-based methods can be highly unreliable. In fact, variations of porosity for Navajo sandstone (11.8%), Weber sandstone (9.5%) and Berea sandstone (17.8%) are only 0.2%, 0.7% and 0.8% porosity units, respectively, for changes of the confining pressure from 0 to 100 MPa, while the corresponding increases in bulk moduli are in the range 15–20 GPa (Coyner 1984; Berryman 1992). The bulk and shear moduli of the sand and clay matrices versus porosity are obtained from a relationship proposed by Krief *et al.* (1990). To obtain the expression of the dry-rock moduli versus effective pressure, the model requires calibration based on well, geological and laboratory data, mainly sonic and density data, and porosity and clay content inferred from logging profiles.

EQUATION OF MOTION

The theory developed by Carcione *et al.* (2000) explicitly takes into account the presence of three phases: sand grains, clay particles and fluids, with $v = 1, 2$ and 3 denoting sand, fluid and clay, respectively. The equation of motion can be written in matrix form as

$$\mathbf{R}\ \text{grad div}\ \mathbf{u} - \boldsymbol{\mu}\ \text{curl curl}\ \mathbf{u} = \boldsymbol{\rho}\ddot{\mathbf{u}} + \mathbf{B}\dot{\mathbf{u}}, \tag{1}$$

where $\mathbf{u}$ is the displacement field,

$$\mathbf{R} = \begin{pmatrix} R_{11} & R_{12} & R_{13} \\ R_{12} & R_{22} & R_{23} \\ R_{13} & R_{23} & R_{33} \end{pmatrix} \quad \text{and} \quad \boldsymbol{\mu} = \begin{pmatrix} \mu_{11} & 0 & \mu_{13} \\ 0 & 0 & 0 \\ \mu_{13} & 0 & \mu_{33} \end{pmatrix} \tag{2}$$

are the bulk and shear stiffness matrices, respectively, while

$$\boldsymbol{\rho} = \begin{pmatrix} \rho_{11} & \rho_{12} & \rho_{13} \\ \rho_{12} & \rho_{22} & \rho_{23} \\ \rho_{13} & \rho_{23} & \rho_{33} \end{pmatrix} \tag{3}$$

is the mass density matrix, and

$$\mathbf{B} = \begin{pmatrix} b_{11} & -b_{11} & b_{13} \\ -b_{11} & b_{11} + b_{33} & -b_{33} \\ b_{13} & -b_{33} & b_{33} \end{pmatrix} \tag{4}$$

is the friction matrix, where b_{13}, which describes interaction between the sand and clay matrices, is a free parameter (no model theory was proposed by Carcione *et al.* 2000). A dot above a variable denotes time differentiation. All the parameters with the subindex (13) describe the interaction between the two solid components. The elements of these matrices are obtained with the use of Lagrange's equations. For brevity, the form of the different coefficients as a function of the

properties of the single constituents is not given here. Their expressions have been given by Carcione *et al.* (2000).

The input quantities that play a role in the generalization to include pressure, attenuation and saturation effects are: the porosity ϕ; the sand fraction ϕ_s; the clay fraction ϕ_c; the clay content C; the dry-rock bulk and shear moduli of the sand matrix, K_{sm} and μ_{sm}, respectively; the coupling modulus between the frame and the fluid, R_{12}; the fluid-mixture bulk modulus, K_f; the fluid-mixture viscosity η_f; the tortuosity for the fluid mixture flowing through the sand matrix $\mathcal{T}_1$; the tortuosity for the fluid mixture flowing through the clay matrix $\mathcal{T}_3$; the permeability of the sand matrix κ_1; the permeability of the clay matrix κ_3; the average diameters of sand and clay particles, d_s and d_c, respectively.

The following relationships hold:

$$\phi + \phi_s + \phi_c = 1 \quad \text{and} \quad C = \frac{\phi_c}{\phi_c + \phi_s}. \tag{5}$$

PORE PRESSURE EFFECTS

We consider the model of Krief *et al.* (1990) to obtain an estimation of the dry-rock moduli K_{sm}, μ_{sm} (sand matrix), K_{cm} and μ_{cm} (clay matrix) versus porosity and clay content. The porosity dependence of the sand and clay matrices should be consistent with the concept of critical porosity, since the moduli should vanish above a certain value of the porosity (usually from 0.4 to 0.5). This dependence is determined by the empirical coefficient A (see equation (6)). This relationship was suggested by Krief *et al.* (1990) and applied to sand/clay mixtures by Goldberg and Gurevich (1998). The bulk and shear moduli of the sand and clay matrices are respectively given by

$$\begin{aligned}
K_{sm}(z) &= K_s[1 - C(z)][1 - \phi(z)]^{1+A/[1-\phi(z)]},\\
K_{cm}(z) &= K_c C(z)[1 - \phi(z)]^{1+A/[1-\phi(z)]},\\
\mu_{sm}(z) &= K_{sm}(z)\mu_s/K_s,\\
\mu_{cm}(z) &= K_{cm}(z)\mu_c/K_c,
\end{aligned} \tag{6}$$

where z is depth, K_s and μ_s are the bulk and shear moduli of the sand grains and K_c and μ_c are those of the clay particles. Krief *et al.* (1990) set the A parameter to 3 regardless of the lithology and Goldberg and Gurevich (1998) obtained values between 2 and 4, while Carcione *et al.* (2000) used $A = 2$. Alternatively, the value of A can be estimated by using regional data from the study area.

We assume the following functional form for the dry-rock moduli as a function of depth and effective pressure:

$$\begin{aligned}
K_{sm}(z,p) &= \beta K_{HS}[1 - \exp(-p_e(p)/p^*_K(z))],\\
\mu_{sm}(z,p) &= \beta \mu_{HS}[1 - \exp(-p_e(p)/p^*_\mu(z))],
\end{aligned} \tag{7}$$

where $p^*(z)$ is obtained (for each modulus) by fitting Krief *et al.*'s (1990) expressions (6). The effective pressure at depth z is assumed to be $p_e = p_c - np$, where p_c is the confining pressure, p is the pore pressure, and the effective stress coefficient $n = 1$, according to Zimmerman (1991, p. 33). Moreover, K_{HS} and μ_{HS} are the Hashin–Shtrikman (HS) upper bounds (Hashin and Shtrikman 1963; Mavko, Mukerji and Dvorkin 1998, p. 106), given by

$$K_{HS}(z) = \left\{ K_s + \phi(z)\left[(1 - \phi(z))\left(K_s + \frac{4}{3}\mu_s\right)^{-1} - K_s^{-1}\right]^{-1} \right\} \tag{8}$$

and

$$\mu_{HS}(z) = \mu_s\left\{ 1 + 5\phi(z)\left[2(1 - \phi(z))(K_s + 2\mu_s)\left(K_s + \frac{4}{3}\mu_s\right)^{-1} - 5\right]^{-1} \right\}. \tag{9}$$

Note that the HS lower bounds are zero, and that the Voigt bounds are $(1 - \phi) K_s$ and $(1 - \phi)\mu_s$, respectively. For quartz grains with clay, $K_s = 39$ GPa and $\mu_s = 33$ GPa (Mavko *et al.* 1998, p. 307), and if the limit porosity is 0.2, the HS upper bounds for the bulk and shear moduli are 26 GPa and 22 GPa, compared with the Voigt upper bounds of 31 GPa and 26 GPa, respectively. However, the HS bounds are too wide to model the moduli of *in situ* rocks. These contain clay and residual water saturation, inducing a chemical weakening of the contacts between grains (Knight and Dvorkin 1992; Mavko *et al.* 1998, p. 203). Therefore, these bounds are multiplied by the parameter $\beta < 1$, which can be obtained by fitting regional data (Carcione *et al.* (2001b) used $\beta = 0.8$).

An alternative evaluation of the dry-rock moduli can be obtained from laboratory experiments. The seismic bulk moduli K_{sm} and μ_{sm} versus confining pressure can be obtained from laboratory measurements on dry samples. If V_P(dry) and V_S(dry) are the experimental compressional and shear velocities, the moduli are given approximately by

$$\begin{aligned}
K_{sm} &= (1 - \phi)\rho_s\left(V_P(\text{dry})^2 - \frac{4}{3}V_S(\text{dry})^2\right),\\
\mu_{sm} &= (1 - \phi)\rho_s V_S(\text{dry})^2,
\end{aligned} \tag{10}$$

where ρ_s is the grain density. We recall that K_{sm} is the rock modulus at constant pore pressure, i.e. the case when the bulk modulus of the pore fluid is negligible compared with the dry-rock bulk modulus, as, for example, air at room

conditions. For $C<0.5$ and $C>0.5$, the clay- and sand-matrix moduli are simply given by Krief *et al.*'s (1990) expressions.

EFFECTIVE FLUID MODEL FOR PARTIAL SATURATION

The mixture hydrocarbon/water behaves as a composite fluid with properties depending on the constants of the constituents and their relative concentrations. This problem has been discussed by Berryman, Thigpen and Chin (1988) and the results are given by the formulae

$$K_{\mathrm{f}}=\left(\frac{S_{\mathrm{g}}}{K_{\mathrm{g}}}+\frac{S_{\mathrm{w}}}{K_{\mathrm{w}}}\right)^{-1} \tag{11}$$

(Wood's law),

$$\rho_{\mathrm{f}}=S_{\mathrm{g}}\rho_{\mathrm{g}}+S_{\mathrm{w}}\rho_{\mathrm{w}} \tag{12}$$

and

$$\eta_{\mathrm{f}}=\eta_{\mathrm{g}}\left(\frac{\eta_{\mathrm{w}}}{\eta_{\mathrm{g}}}\right)^{S_{\mathrm{w}}} \tag{13}$$

(Teja and Rice 1981a,b), where K_{g} and K_{w}, ρ_{g} and ρ_{w}, η_{g} and η_{w}, S_{g} and S_{w} are the bulk moduli, densities, viscosities and saturations of hydrocarbon and water, respectively. In the examples, we compare (13) to the linear law $\eta_{\mathrm{f}}=S_{\mathrm{w}}\eta_{\mathrm{w}}+S_{\mathrm{g}}\eta_{\mathrm{g}}$.

Equation (11) corresponds to the low-frequency range. When the fluids are not mixed in the pore volume, but distributed in patches, the effective bulk modulus of the fluid mixture at high frequencies is higher than that predicted by (11). We use an empirical mixing law introduced by Brie *et al.* (1995). The effective fluid bulk modulus is given by

$$K_{\mathrm{f}}=(K_{\mathrm{w}}-K_{\mathrm{g}})S_{\mathrm{w}}^{e}+K_{\mathrm{g}}, \tag{14}$$

where $e=(f_0/f)^{0.34}$ is an empirical parameter, with f_0 being a reference frequency. The exponent 0.34 fits the sonic-band data provided by Brie *et al.* (1995). Equation (14) gives Voigt's mixing law for $e=1$ and Wood's law for $e=40$.

In the case of gas saturation, the gas density and bulk modulus as a function of pressure and temperature are calculated using van der Waals' equation (see Carcione and Gangi 2000b).

PERMEABILITY AND PARTIAL SATURATION

The acoustic model requires partial permeabilities. The permeability for a rock of mixed particle size can be expressed by the Kozeny–Carman relationship (Dullien 1991),

$$\kappa=B(\phi-\phi_p)^3\overline{d}^2\mathcal{T}^{-1}, \tag{15}$$

where B is a geometrical factor, $\mathcal{T}$ is the tortuosity of the mixture and $\overline{d}$ is the effective grain size defined by

$$\overline{d}=\left(\frac{1-C}{d_1}+\frac{C}{d_3}\right)^{-1}, \tag{16}$$

with d_1 and d_3 being the grain diameter of the sand and clay particles, respectively. Following Mavko and Nur (1997), we have introduced a percolation porosity ϕ_{p}. The tortuosity is given by

$$\mathcal{T}=\left(\frac{1-C}{\mathcal{T}_1}+\frac{C}{\mathcal{T}_3}\right)^{-1}. \tag{17}$$

Equation (17) indicates that the tortuosity of the rock can be obtained by using an analogy with electric circuits. It is given by a parallel connection of resistances, where the resistances are the tortuosity through the sand matrix, $\mathcal{T}_\infty$, and the tortuosity through the clay matrix, $\mathcal{T}_\epsilon$. We then have $\mathcal{T}<\mathcal{T}_\infty$ and $\mathcal{T}<\mathcal{T}_\epsilon$. This analogy uses the fact that increasing tortuosity increases the resistance to fluid flow.

Carcione *et al.* (2000) obtained the following expressions for the partial permeabilities:

$$\kappa=\kappa_1\phi_{\mathrm{s}}+\kappa_3\phi_{\mathrm{c}} \tag{18}$$

and

$$\frac{\kappa_3}{\kappa_1}=\left(\frac{d_3}{d_1}\right)^2\left(\frac{\phi_{\mathrm{s}}}{\phi_{\mathrm{c}}}\right). \tag{19}$$

For a partially saturated medium, the effective permeability is given by the following generalization of (15):

$$\kappa=B(\phi-\phi_p)^3\overline{d}^2\mathcal{T}^{-1}[\kappa_{\mathrm{rw}}S_{\mathrm{w}}+\kappa_{\mathrm{rg}}(1-S_{\mathrm{w}})], \tag{20}$$

where κ_{rw} and κ_{rg} are normalized relative permeabilities given by

$$\kappa_{\mathrm{rw}}=\sqrt{S_{\mathrm{we}}}[1-(1-S_{\mathrm{we}}^{1/m_{\mathrm{w}}})^{m_{\mathrm{w}}}]^2,\quad S_{\mathrm{we}}=\frac{S_{\mathrm{w}}-S_{\mathrm{wi}}}{1-S_{\mathrm{wi}}}, \tag{21}$$

and

$$\kappa_{\mathrm{rg}}=\sqrt{S_{\mathrm{ge}}}[1-(1-S_{\mathrm{ge}}^{1/m_{\mathrm{g}}})^{m_{\mathrm{g}}}]^2,\quad S_{\mathrm{ge}}=\frac{S_{\mathrm{g}}-S_{\mathrm{gi}}}{1-S_{\mathrm{gi}}} \tag{22}$$

(Van Genuchten 1978; Bear and Bachmat 1990, p. 360). In (21) and (22), S_{wi} and S_{gi} are the irreducible water saturation and entrapped gas, respectively (Bear and Bachmat 1990, p. 344) and we set $m_{\mathrm{w}}=1.1$ and $S_{\mathrm{wi}}=0.2$ for water, and $m_{\mathrm{g}}=1.5$ and $S_{\mathrm{gi}}=0.1$ for gas by fitting experimental data from a North Sea reservoir (Fig. 2a). The partial permeabilities are then obtained from (18), (19) and (20). Equation (20)

is not restricted to any particular model of the pore space. The information about the pore geometry and grain sizes is contained in the parameters B, $\overline{d}$ and $\mathcal{T}$. This description of permeability assumes an even distribution of the clay particles in the elementary volume. In this sense, the description is consistent with the model of interpenetrating sand and clay matrices on which the Biot-type theory of Carcione *et al.* (2000) is based.

ATTENUATION AND VISCODYNAMIC EFFECTS

In natural porous media such as sandstone, discrepancies between Biot theory and measurements are due to complex pore shapes and the presence of clay, which are not present in synthetic media. This complexity gives rise to a variety of relaxation mechanisms that contribute to the attenuation of the different wave modes. Stoll and Bryan (1970) showed that attenuation is controlled by the anelasticity of the skeleton (friction at grain contacts) and by viscodynamic causes. The latter involve local (squirt) flow and global (Biot) flow. Global flow is implicit in Biot's theory and squirt flow is modelled by using a single relaxation mechanism based on the Zener model (Bourbié, Coussy and Zinszner 1987, p. 227; Dvorkin, Nolen-Hoekksema and Nur 1994; Carcione 1998, 2001b, p. 65).

Losses due to scattering are not explicitly described by the present model, which is based on an effective-medium theory (the wavelength of the signal is much larger than the pore size). However, when laboratory measurements and sonic logs are used to infer the behaviour of acoustic properties at seismic frequencies, the frequency dependence of these properties is a key factor. As demonstrated by White (1975), wave velocity and attenuation are substantially affected by the presence of partial (patchy) saturation, mainly depending on the size of the gas pockets (saturation), frequency and permeability. These effects are implicitly described by Biot-type theories, when using full-wave modelling codes to obtain synthetic seismograms in inhomogeneous media.

Constant-Q models provide a simple parametrization of seismic attenuation in rocks in oil exploration and in seismology. By reducing the number of parameters they allow an improvement in seismic inversion. Moreover, there is physical evidence that attenuation is almost linear with frequency (therefore Q is constant) in many frequency bands. Bland (1960) and Kjartansson (1979) discussed a linear attenuation model with the required characteristics, but the idea is much older (Scott-Blair 1949).

The constant-Q kernel is the simplest model based on only one parameter. Keller (1989) used this kernel to model frame anelasticity in Biot's theory for isotropic saturated media. He obtained a good fit of experimental P-wave attenuation and velocity of sediments. The attenuation kernel corresponding to a constant Q over all frequencies is

$$M(\omega, Q) = \left(\frac{\mathrm{i}\omega}{\omega_0}\right)^{2\gamma}, \quad \gamma = \frac{1}{\pi}\tan^{-1}\left(\frac{1}{Q}\right), \tag{23}$$

where ω_0 is a reference frequency. Attenuation is modelled by making the frame bulk and shear moduli viscoelastic, where by frame we mean the sandstone skeleton. Then,

$$K_{\mathrm{sm}} \to K_{\mathrm{sm}} M(\omega, Q_K), \tag{24}$$

where

$$Q_K = \frac{K_{\mathrm{sm}}(z,p)}{K_{\mathrm{sm}}(z)} Q_0, \tag{25}$$

where Q_0 is the given loss parameter for the sand skeleton, and $K_{\mathrm{sm}}(z)$ is given by (6) for a reference rock with porosity ϕ_0 and clay content C_0 at a reference pressure p_0. $K_{\mathrm{sm}}(z,p)$ is given by (7). The corresponding Q factors for the shear and coupling moduli are given by

$$Q_\mu = \frac{\mu_{\mathrm{sm}}(z,p)}{K_{\mathrm{sm}}(z,p)} Q_K \quad \text{and} \quad Q_R = \frac{R_{12}(z,p)}{K_{\mathrm{sm}}(z,p)} Q_K, \tag{26}$$

and

$$\mu_{\mathrm{sm}} \to \mu_{\mathrm{sm}} M(\omega, Q_\mu) \quad \text{and} \quad R_{12} \to R_{12} M(\omega, Q_R). \tag{27}$$

Equations (26) imply that the lower the modulus, the higher the attenuation.

High-frequency viscodynamic effects imply the substitution in (4),

$$b_{ii} = \left(\frac{\eta_{\mathrm{f}}\phi^2}{\kappa_i}\right) F_i(\omega), \quad i = 1, 3, \tag{28}$$

where F_1 and F_3 are viscodynamic functions corresponding to the interaction between the sand and clay matrices with the fluid, respectively (Biot 1962). Johnson *et al.* (1987) obtained an expression for the viscodynamic function, which provides a good description of both the magnitude and phase of the exact dynamic tortuosity of large networks formed from a distribution of random radii.

The viscodynamic function is

$$F_i(\omega) = \sqrt{1 - \mathrm{i}\frac{4\mathcal{T}_i^2 \kappa_i}{x_i L_i^2 \phi}}, \quad x_i = \frac{\eta_{\mathrm{f}}\phi}{\omega \kappa_i \rho_{\mathrm{f}}}, \quad i = 1, 3, \tag{29}$$

where κ_i are permeabilities, defined by Carcione *et al.* (2000), and L_i is a geometrical parameter, with $2/L_i$ being the surface-to-pore volume ratio of the pore/solid interface. The following relationship between $\mathcal{T}_i$, κ_i and L_i can be used: $\xi_i \mathcal{T}_i \kappa_i / \phi L_i^2 = 1$, where ξ_i describes the shape of the pore network, with values $\xi_i = 12$ for a set of canted slabs of fluid and $\xi_i = 8$ for a set of non-intersecting canted tubes.

PHASE VELOCITY AND QUALITY FACTOR

The three compressional velocities of the three-phase porous medium are given by

$$V_{Pm} = \left[\mathrm{Re}\left(\sqrt{\Lambda_m}\right)\right]^{-1}, \quad m = 1, 2, 3, \tag{30}$$

where Re denotes the real part, and Λ_m are obtained from the generalized characteristic equation, $\det(\Lambda \mathbf{R} - \tilde{\boldsymbol{\rho}}) = 0$, which yields

$$\Lambda^3 \det(\mathbf{R}) - \Lambda^2 \mathrm{tr}(\bar{\mathbf{R}}\tilde{\boldsymbol{\rho}}) + \Lambda\ \mathrm{tr}(\mathbf{R}\bar{\tilde{\boldsymbol{\rho}}}) - \det\tilde{\boldsymbol{\rho}} = 0,$$

where tr is the trace, the overbar denotes the cofactor matrix (e.g. Fedorov 1968), and the effective density matrix,

$$\tilde{\boldsymbol{\rho}} = \boldsymbol{\rho} - \mathrm{i}\mathbf{B}/\omega,$$

is defined in the frequency domain.

Similarly, the two shear velocities V_{Sm} are given by

$$V_{Sm} = \left[\mathrm{Re}\left(\sqrt{\Omega_m}\right)\right]^{-1}, \quad m = 1, 2, \tag{31}$$

where Ω_m are the complex solutions of the equation,

$$\Omega^2 \mathrm{tr}(\bar{\boldsymbol{\mu}}\tilde{\boldsymbol{\rho}}) - \Omega \mathrm{tr}(\boldsymbol{\mu}\bar{\tilde{\boldsymbol{\rho}}}) + \det(\tilde{\boldsymbol{\rho}}) = 0.$$

The P and S quality factors for homogeneous viscoelastic plane waves are given by the following approximations:

$$Q_{Pm} = -\frac{\mathrm{Re}(\Lambda_m)}{\mathrm{Im}(\Lambda_m)}, \quad m = 1, 2, 3, \tag{32}$$

and

$$Q_{Sm} = -\frac{\mathrm{Re}(\Omega_m)}{\mathrm{Im}(\Omega_m)}, \quad m = 1, 2 \tag{33}$$

(Carcione 2001a).

EXAMPLES

We consider a sandstone saturated with water and gas. Table 1 shows the properties of the different constituents. The porosity in most of the examples is $\phi = 0.246$ (Berea sandstone, see King, Marsden and Dennis 2000) and the value of the other quantities are as follows: the effective stress coefficient $n_K = 0.75$ at $p_d = 40$ MPa; Krief *et al.*'s (1990) parameter $A = 2.8$; the diameters of the sand and clay particles, $d_s = 0.1$ mm and $d_c = 2\,\mu$m; residual saturations, $S_{wg} = 0.4$ and $S_{gw} = 0.1$; the reference frequency in Brie *et al.*'s (1995) equation, $f_0 = 1$ MHz; the percolation porosity, $\phi_p = 3.5\%$; the geometrical factor in the Kozeny–Carman equation, $B = 15$; the relative permeability parameters, $m_w = 0.8$ and $m_g = 1.8$; the loss parameters, $Q_0 = 60$ and $\omega_0 = 2\pi$ MHz; the friction coefficient, $b_{13} = 0$; and the parameters describing the shape of the pore network, $\xi_1 = \xi_3 = 8$.

Table 1 Material properties of the clay-bearing sandstone

Sand	Bulk modulus, K_s	35 GPa
	Shear modulus, μ_s	35 GPa
	Density, ρ_s	2650 kg/m^3
	Average diameter, d_s	100 μm
Clay	Bulk modulus, K_c	20 GPa
	Shear modulus, μ_c	10 GPa
	Density, ρ_c	2650 kg/m^3
	Average diameter, d_c	2 μm
Pore fill	Bulk modulus, K_w	2.4 GPa
	Density, ρ_w	1030 kg/m^3
	Viscosity, η_w	1.798 cP
	Bulk modulus, K_g	0.01 GPa
	Density, ρ_g	100 kg/m^3
	Viscosity, η_g	0.02 cP

Figure 1 shows the tortuosity (a) and the permeability (b) (equation (15)) versus porosity and clay content, for various values of the clay content and porosity, respectively. We fit experimental data published by Klimentos and McCann (1990) (their Table 1, and plotted in their Fig. 23) (permeability versus clay content). Our plot is on a log–linear scale while their plot is on a linear–linear scale, hence the scatter in the data is more prominent in our Fig. 1(b) than in their Fig. 23. In general, permeability (and porosity) data from core measurements reveal a scattered appearance; the reasons for this are several (Worthington 1991) but mainly related to the core handling and the methods of measurements. This problem was also discussed by Helle, Bhatt and Ursin (2001). In view of this, we consider the fit of our model to the data to be acceptable. Note the strong decrease in permeability due to the addition of a small amount of clay. The normalized relative permeabilities (a) and the viscosity of the water/gas mixture (b) are shown in Fig. 2 as a function of water saturation. Both permeabilities decrease for decreasing saturation of the corresponding fluid. In particular, there is practically no water flow below 50% water saturation. Figure 2(b) compares the linear mixing law (dashed line)

with the more realistic mixing law of Teja and Rice (1981a, b) (continuous line). The linear relationship overestimates the viscosity of the mixture. Figure 3 shows the bulk modulus of the water/gas mixture versus water saturation (a) and frequency (b). Brie *et al.*'s (1995) model is in good agreement with the Voigt and Wood bounds.

Figure 4(a, b) compare the P- and S-wave velocities predicted by our model with experimental data obtained by King *et al.* (2000). In (b), the velocities are represented for several frequencies, from the seismic to the ultrasonic band. The P-wave velocity obtained by using Hill's equation (Mavko *et al.* 1998, p. 115) is also shown. We average the reciprocal of the P-wave modulus (ρV_P^2) in the absence of attenuation. The use of Brie *et al.*'s (1995) model, although empirical, allows us to model the acoustic properties of the sandstone in the whole frequency range. It must be emphasized that not every input parameter has been measured, so no prediction in the conventional sense has been made.

Three-dimensional plots of the P-wave velocity (a) and the dissipation factor (b) versus differential pressure (confining pressure minus pore pressure) and water saturation are shown in Fig. 5. The clay content is 5% and the frequency is 30 Hz.

As in Carcione (1998), we have modelled the squirt-flow mechanisms with a single relaxation peak based on the Zener mechanical model. The generalization of the coupling modulus M in Carcione (1998) is K_{av} in Carcione *et al.* (2000). This modulus is generalized to a complex Zener modulus

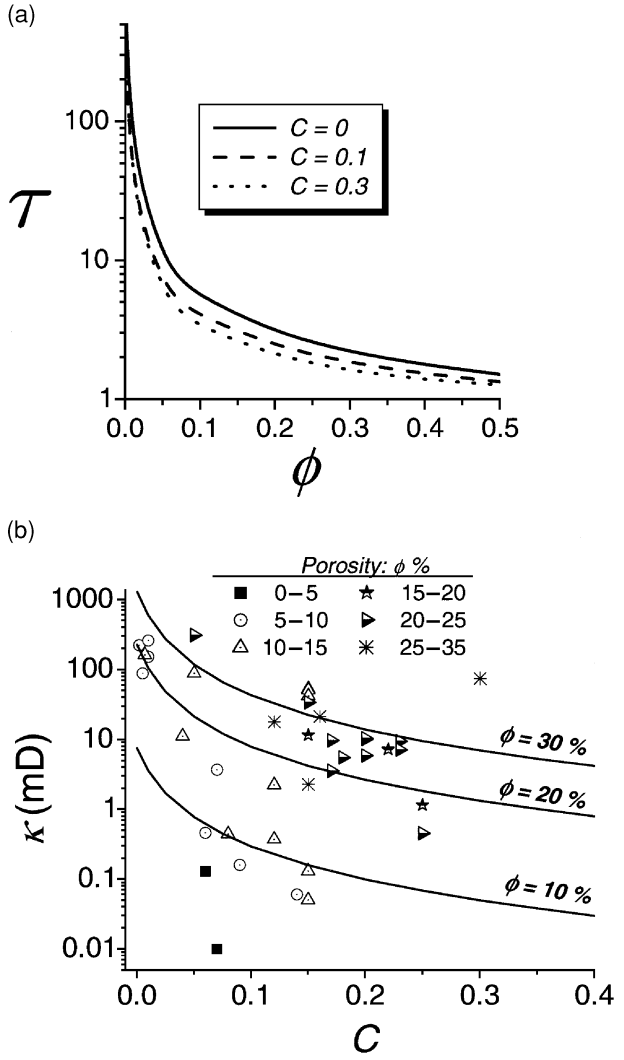

Figure 1 Tortuosity (a) and permeability (b) versus porosity and clay content. The experimental data are taken from Klimentos and McCann (1990).

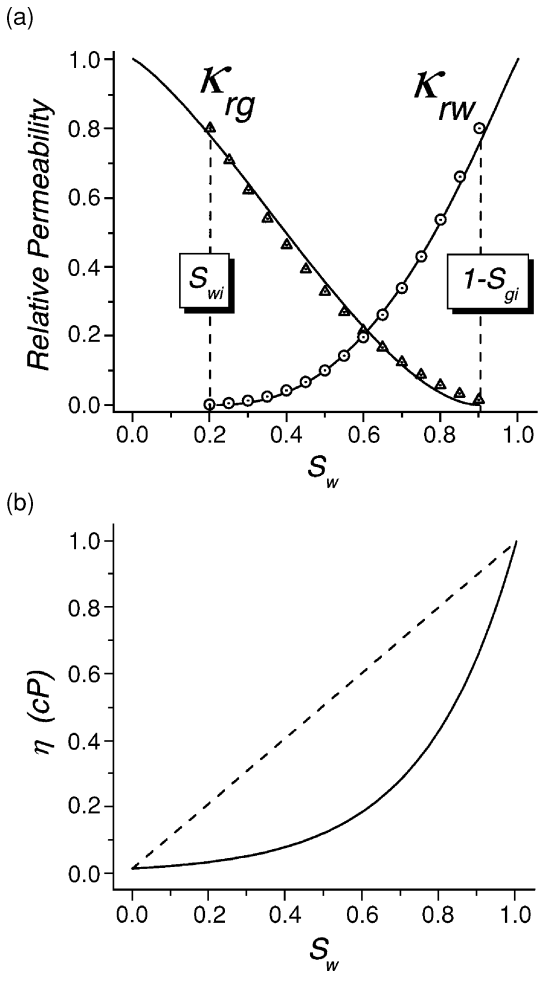

Figure 2 Fitted curves of normalized relative permeabilities using data from a North Sea reservoir (a) and viscosity of the water/gas mixture (b) as a function of water saturation. The dashed line is the linear viscosity law.

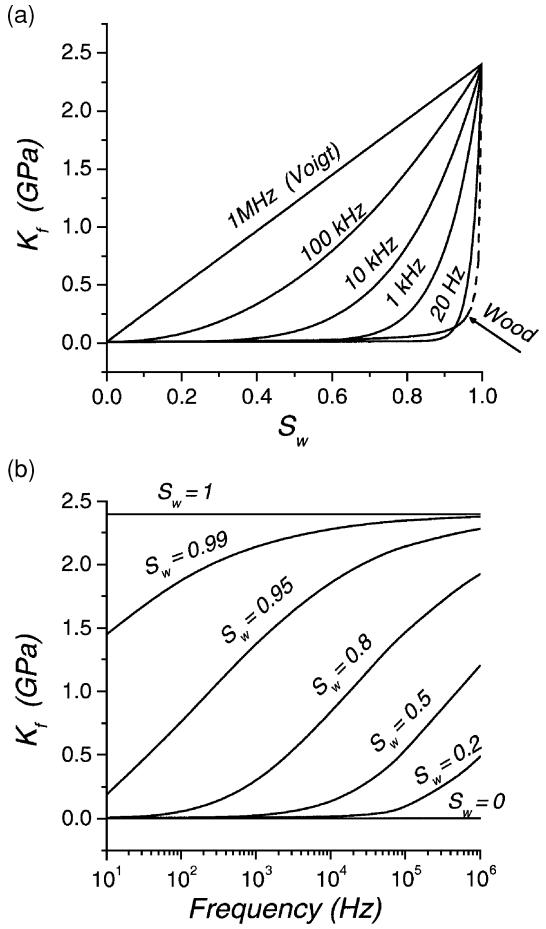

Figure 3 Bulk modulus of the water/gas mixture versus water saturation (a) and frequency (b).

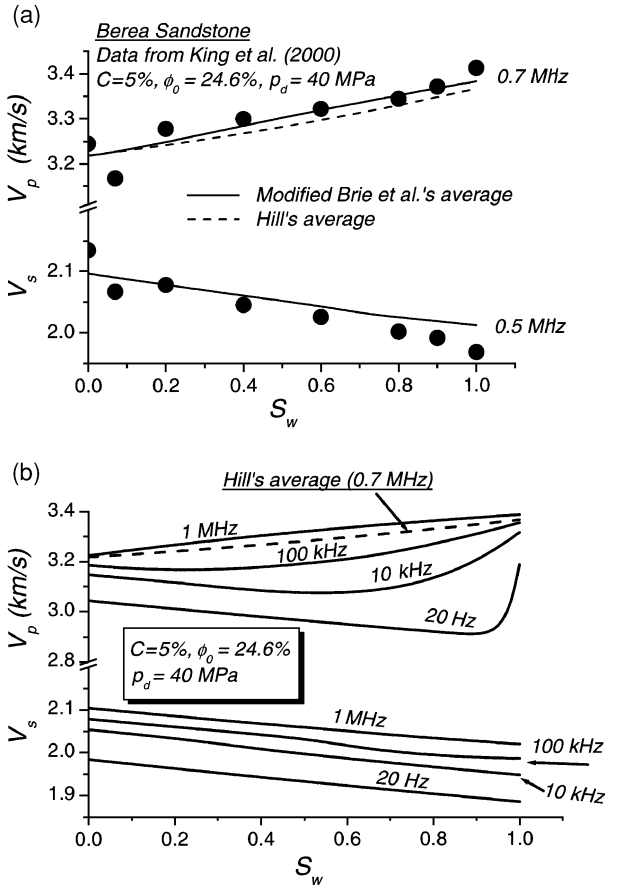

Figure 4 (a) P- and S-wave velocities predicted by the present model compared with the experimental data of King *et al.* (2000) at ultrasonic frequencies. (b) The same properties as in (a) but for all frequencies. The P-wave velocity obtained by using Hill's equation is also shown (dashed line).

(e.g. Carcione 2001b, p. 65). For partial saturation, the centre of the peak is given by

$$f_0 = f_{0g}(1 - S_w) + f_{0w} S_w, \tag{34}$$

where $f_{0g} = 40$ kHz and $f_{0w} = 3$ kHz. The maximum quality factors associated with gas and water are equal to 10 for both fluids.

Note the strong decrease in the velocity and the Q factor with decreasing differential pressure (Fig. 5b). This effect is mainly due to the fact that the dry-rock moduli are sensitive functions of the effective pressure. (At very low effective pressures, the rock becomes unconsolidated.) Figure 6 shows the same properties as in Fig. 5, but versus water saturation and frequency. In this case, the differential pressure is 40 MPa ($p_c = 70$ MPa and $p = 30$ MPa), and we assume that the temperature is 90 °C in van der Waals' equation (Carcione and Gangi 2000b), corresponding to a reservoir at 3 km depth. Figure 6(b) agrees qualitatively with a similar plot, based on experimental data from Massilon sandstone, published by Murphy (1982). The dissipation factor has a maximum value at the squirt-flow relaxation peak. A secondary maximum corresponds to the Biot peak. The losses at full water saturation are stronger than the losses at full gas saturation. The behaviour of attenuation agrees qualitatively with experimental data published by Yin, Batzle and Smith (1992).

The S-wave velocity and the S-wave dissipation factor as a function of saturation and frequency are shown in Figs 7(a) and (b), respectively. The S-wave velocity increases with frequency and, in general, with decreasing water saturation. Attenuation has a maximum at approximately the location of the Biot peak and 100% water saturation.

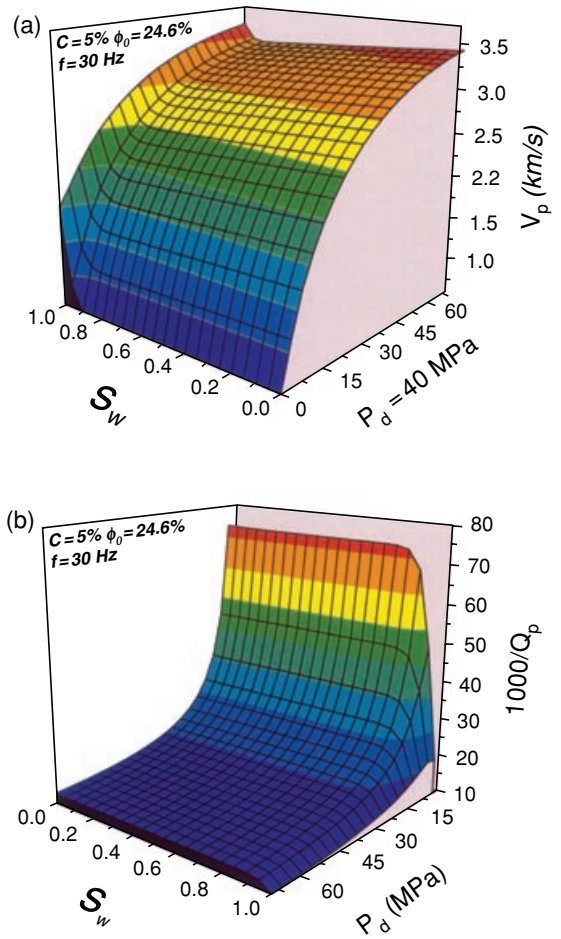

Figure 5 Three-dimensional plots of P-wave velocity (a) and dissipation factor (b) versus differential pressure (confining pressure minus pore pressure) and water saturation. The clay content is 5%, the helium core porosity is 24.6% (at atmospheric pressure) and the frequency is 30 Hz.

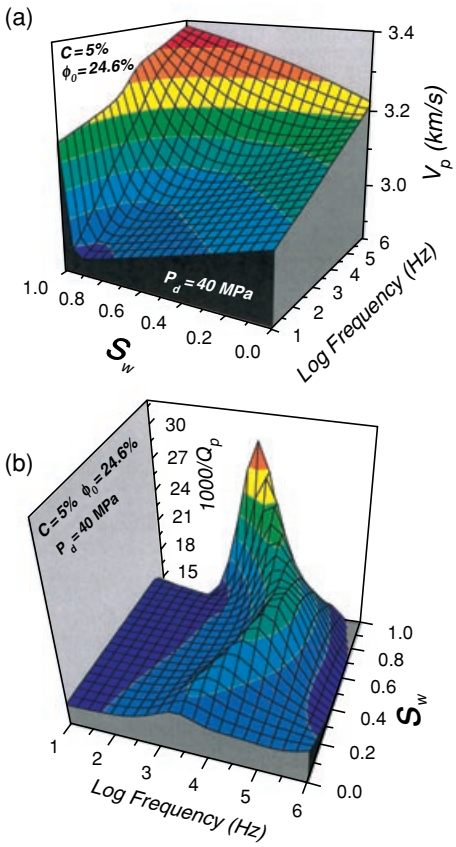

Figure 6 Three-dimensional plots of the P-wave velocity (a) and dissipation factor (b) versus water saturation and frequency. The clay content is 5%, the helium core porosity is 24.6% and the differential pressure is 40 MPa.

Figure 8 shows the wave velocities (a) and the dissipation factors (b) and (c) versus water saturation and different values of the clay content C at 10 kHz. The permeability corresponding to each value of C is indicated on the curves. In general, attenuation increases with increasing clay content and decreasing permeability (decreasing fluid-flow length). Finally, the 3D plots in Figs 9 and 10 show more clearly the effect of clay and saturation on the dissipation factors for frequencies of 10 kHz (a), 100 kHz (b) and 1 MHz (c).

In the sonic range, we can see the Biot relaxation peak for high gas saturation and high clay content, and the squirt-flow peak at high water saturation (a). The linear increase in attenuation at full water saturation and 1 MHz agrees with the empirical equation obtained by Klimentos and McCann (1990). The Biot peak gradually moves towards higher water saturation as the frequency increases (b and c), while the squirt-flow peak disappears. Moreover, at higher frequencies (c), the attenuation reveals stronger dependence on the clay content at high water saturation. For a fully saturated rock ($S_w = 1$) at 1 MHz, i.e. under standard laboratory conditions, the attenuation increases monotonously with the clay content (c), in agreement with the experimental results of Klimentos and McCann (1990) and Best, McCann and Sothcott (1994).

The presence of clay increases the surface area and decreases the permeability, increasing the attenuation of the slow wave (Klimentos and McCann 1988). Furthermore, the presence of the slow wave constitutes an attenuation mechanism for the fast P-wave, due to mode conversion at heterogeneities. This effect is implicit in the computation of synthetic seismograms when using a full-wave modelling method (e.g. Carcione 1998).

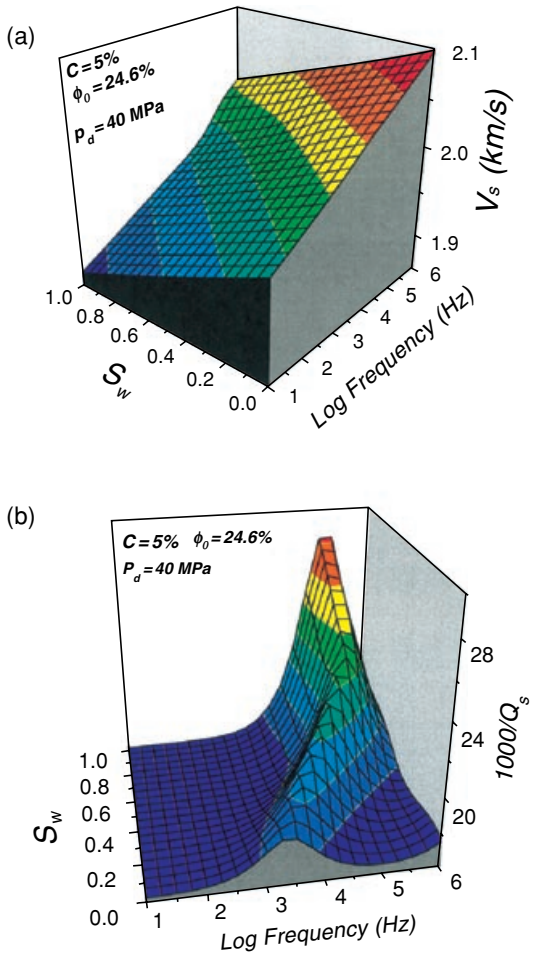

Figure 7 As Fig. 5 but for S-waves.

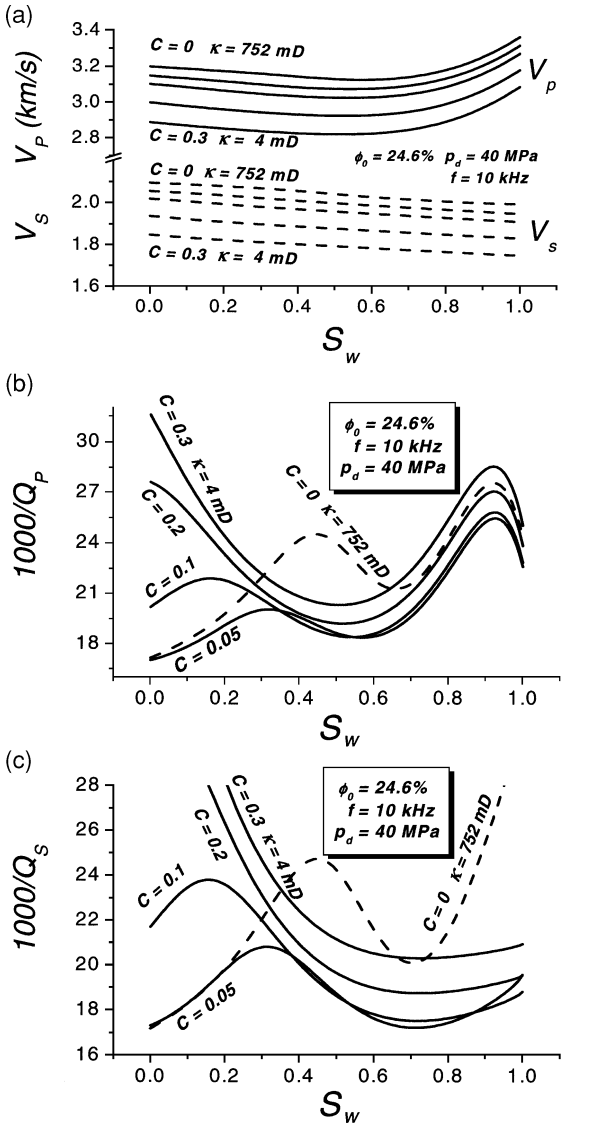

Figure 8 Wave velocities (a) and dissipation factors (b and c) versus water saturation for different values of the clay content C at a frequency of 10 kHz. The permeability corresponding to each value of C is indicated on the curves.

CONCLUSIONS

We have developed a model of the acoustic properties – wave velocity and quality factor – of sandstone as a function of clay content, pore pressure, frequency and partial saturation. The theory includes poroviscoelasticity and viscodynamic effects to model the realistic attenuation values observed in rocks from low to high frequencies. The limitations of the model are mainly with regard to the use of the constant-Q model to describe attenuation mechanisms, which are not of viscodynamic nature (local and global fluid-flow losses). However, this limitation is a consequence of the absence of experimental data in the sonic and seismic bands. The constant-Q model could be substituted by a generalized Zener model (parallel or series connection of Zener elements), which can be used to fit a general functional behaviour of quality factor (and velocity dispersion) versus frequency. In this sense, the model is not a predicting tool. Furthermore, the model requires calibration to obtain estimates of the dry-rock moduli and geometrical features of the pore space, such as tortuosity, grain size and permeability.

The model predicts the behaviour of real sandstones in many respects. For instance: (i) There is a strong decrease in permeability due to the addition of a small amount of clay. (ii) Wave velocity increases considerably at high frequencies compared with low frequencies (at low frequencies, the fluid has enough time to achieve pressure equilibration, while at high frequencies, the fluid cannot relax and the bulk and

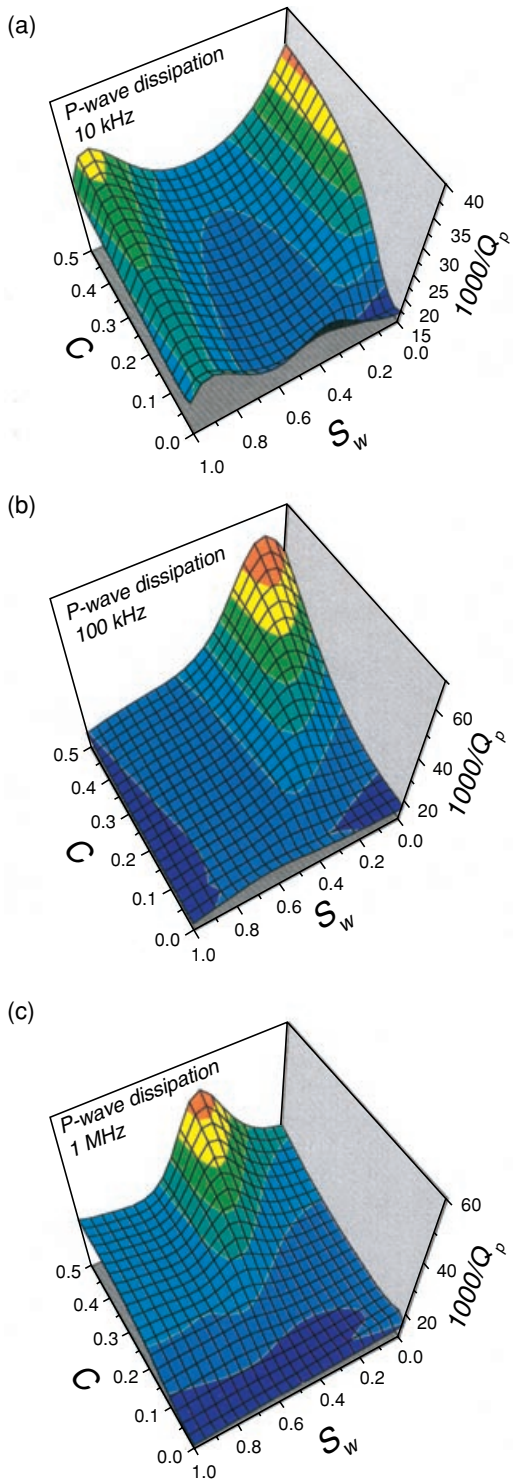

Figure 9 Three-dimensional plots of P-wave dissipation factor versus water saturation S_w and clay content C for 10 kHz (a), 100 kHz (b) and 1 MHz (c). Porosity $\phi = 24.6\%$ and differential pressure $p_d = 40$ MPa.

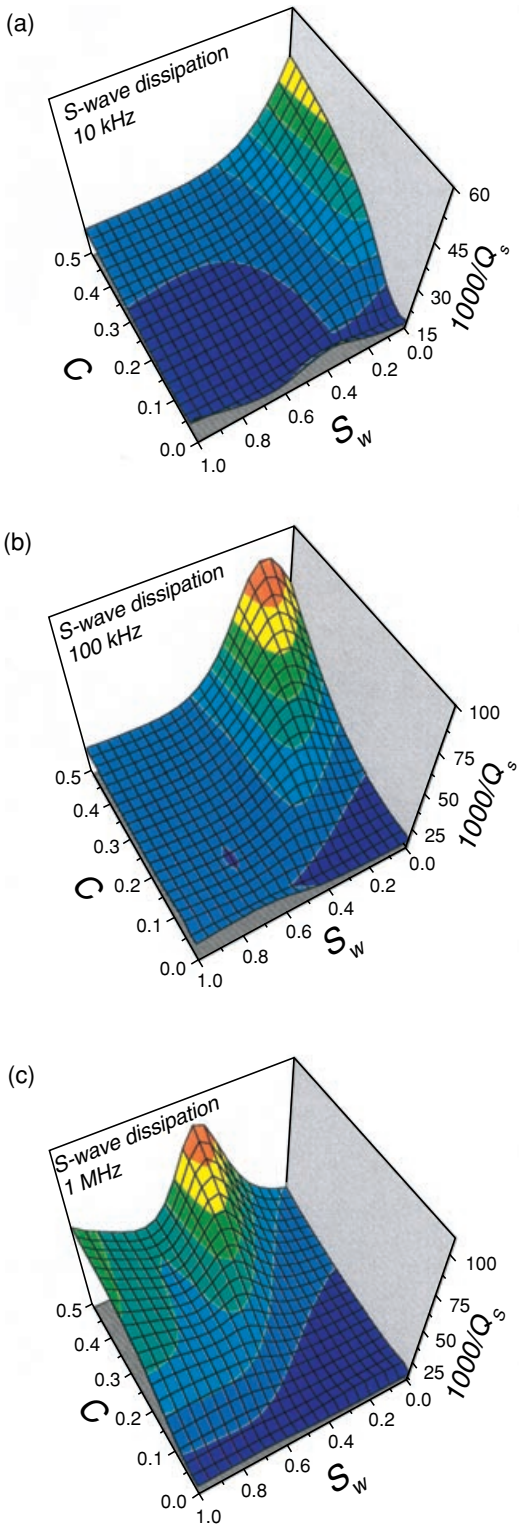

Figure 10 As Fig. 9 but for S-waves.

shear moduli are stiffer than at low frequencies). (iii) There is a strong decrease in the velocity and the Q factor with decreasing differential pressure (this effect is mainly due to the fact that the dry-rock moduli are sensitive functions of the effective pressure). (iv) For a Berea sandstone the attenuation has a maximum at approximately the location of the Biot peak and 90% water saturation. (v) In general, attenuation increases with increasing clay content and decreasing permeability (decreasing fluid-flow length). However, attenuation is strongly dependent on both clay content and fluid saturation. For a shaley sandstone with gas, the attenuation has a peak in the sonic frequency band, while the partially saturated sample has its relaxation peak at ultrasonic frequencies.

ACKNOWLEDGEMENT

This work was in part supported by the European Union under the project 'Detection of overpressure zones with seismic and well data' and by the Norwegian Research Council under the PetroForsk programme (N.H.P.).

REFERENCES

Bear J. and Bachmat Y. 1990. *Introduction to Modeling of Transport Phenomena in Porous Media*. Kluwer Academic Publishers.

Berryman J.G. 1992. Effective stress for transport properties of inhomogeneous porous rock. *Journal of Geophysical Research* **97**, 17409–17424.

Berryman J.G., Thigpen L. and Chin R.C.Y. 1988. Bulk wave propagation for partially saturated porous solids. *Journal of the Acoustical Society of America* **84**, 360–373.

Best A.I., McCann C. and Sothcott J. 1994. The relationships between the velocities, attenuation and petrophysical properties of reservoir sedimentary rocks. *Geophysical Prospecting* **42**, 151–178.

Biot M.A. 1962. Mechanics of deformation and acoustic propagation in porous media. *Journal of Applied Physics* **33**, 1482–1498.

Bland D.R. 1960. *The Theory of Linear Viscoelasticity*. Pergamon Press, Inc.

Bourbié T., Coussy O. and Zinszner B. 1987. *Acoustics of Porous Media*. Éditions Technip.

Brie A., Pampuri F., Marsala A.F. and Meazza O. 1995. Shear sonic interpretation in gas-bearing sands. SPE Annual Technical Conference #30595, 701–710.

Cadoret T., Marion D. and Zinszner B. 1995. Influence of frequency and fluid distribution on elastic wave velocities in partially saturated limestones. *Journal of Geophysical Research* **100**, 9789–9803.

Carcione J.M. 1998. Viscoelastic effective rheologies for modelling wave propagation in porous media. *Geophysical Prospecting* **46**, 249–270.

Carcione J.M. 2001a. Energy balance and fundamental relations in dynamic anisotropic poro-viscoelasticity. *Proceedings of the Royal Society of London A* **457**, 331–348.

Carcione J.M. 2001b. Wave fields in real media: wave propagation in anisotropic, anelastic and porous media. *Handbook of Geophysical Exploration* **31**. Pergamon Press, Inc.

Carcione J.M., Cavallini F., Mainardi F. and Hanyga A. 2001a. Time-domain seismic modeling of constant-Q wave propagation using fractional derivatives. *PAGEOPH* **159**, 1719–1736.

Carcione J.M. and Gangi A. 2000a. Non-equilibrium compaction and abnormal pore-fluid pressures: effects on seismic attributes. *Geophysical Prospecting* **48**, 521–537.

Carcione J.M. and Gangi A. 2000b. Gas generation and overpressure: effects on seismic attributes. *Geophysics* **65**, 1769–1779.

Carcione J.M., Gurevich B. and Cavallini F. 2000. A generalized Biot–Gassmann model for the acoustic properties of clayey sandstones. *Geophysical Prospecting* **48**, 539–557.

Carcione J.M., Helle H.B., Pham N.H. and Toverud T. 2001b. Pore pressure estimation from seismic reflection data. *Geophysics*, in press.

Coyner K.B. 1984. *Effects of stress, pore pressure, and pore fluids on bulk strain, velocity, and permeability of rocks*. PhD thesis, MIT, Cambridge, MA.

Dullien F.A.L. 1991. One and two phase flow in porous media and pore structure. In: *Physics of Granular Media* (eds D. Bideau and J. Dodds), pp. 173–214. Science Publishers, Inc., New York.

Dvorkin J., Nolen-Hoeksema R. and Nur A. 1994. The squirt-flow mechanism: macroscopic description. *Geophysics* **59**, 428–438.

Fedorov F.I. 1968. *Theory of Elastic Waves in Crystals*. Plenum Press.

Goldberg I. and Gurevich B. 1998. A semi-empirical velocity-porosity-clay model for petrophysical interpretation of P- and S-velocities. *Geophysical Prospecting* **46**, 271–285.

Hashin Z. and Shtrikman S. 1963. A variational approach to the elastic behaviour of multiphase materials. *Journal of the Mechanics and Physics of Solids* **11**, 127–140.

Helle H.B., Bhatt A. and Ursin B. 2001. Porosity and permeability from wireline logs using artificial neural networks: a North Sea case study. *Geophysical Prospecting* **49**, 431–444.

Hudson J.A. 1988. Seismic wave propagation through materials containing partially saturated cracks. *Geophysical Journal International* **92**, 33–37.

Hudson J.A., Liu E. and Crampin S. 1996. The mechanical properties of materials with interconnected cracks and pores. *Geophysical Journal International* **124**, 105–112.

Johnson D.L., Koplik J. and Dashen R. 1987. Theory of dynamic permeability and tortuosity in fluid-saturated porous media. *Journal of Fluid Mechanics* **176**, 379–402.

Keller J.D. 1989. Acoustic wave propagation in composite fluid-saturated media. *Geophysics* **54**, 1554–1563.

King M.S., Marsden J.R. and Dennis J.W. 2000. Biot dispersion for P- and S-wave velocities in partially and fully saturated sandstones. *Geophysical Prospecting* **48**, 1075–1089.

Kjartansson E. 1979. Constant-Q wave propagation and attenuation. *Journal of Geophysical Research* **84**, 4737–4748.

Klimentos T. and McCann C. 1988. Why is the Biot slow compressional wave not observed in real rocks? *Geophysics* **12**, 1605–1609.

Klimentos T. and McCann C. 1990. Relationships among compressional wave attenuation, porosity, clay content, and permeability in sandstones. *Geophysics* **55**, 998–1014.

Knight R. and Dvorkin J. 1992. Seismic and electrical properties of sandstones at low saturations. *Journal of Geophysical Research* **97**, 17425–17432.

Krief M., Garat J., Stellingwerff J. and Ventre J. 1990. A petrophysical interpretation using the velocities of P and S waves (full waveform sonic). *The Log Analyst* **31**, 355–369.

Mavko G. and Mukerji T. 1998. Bounds on low-frequency seismic velocities in partially saturated rocks. *Geophysics* **63**, 918–924.

Mavko G., Mukerji T. and Dvorkin J. 1998. *The Rock Physics Handbook: Tools for Seismic Analysis in Porous Media*. Cambridge University Press.

Mavko G. and Nur A. 1997. Effect of a percolation threshold in the Kozeny–Carman relation. *Geophysics* **62**, 1480–1482.

Murphy W.F. 1982. Effect of partial water saturation on attenuation of Massilon sandstone and Vycor porous glass. *Journal of the Acoustical Society of America* **71**, 1458–1468.

Pointer T., Liu E. and Hudson J.A. 2000. Seismic wave propagation in cracked porous media. *Geophysical Journal International* **142**, 199–231.

Scott-Blair G.W. 1949. *Survey of General and Applied Rheology*. Pitman.

Stoll R.D. and Bryan G.M. 1970. Wave attenuation in saturated sediments. *Journal of the Acoustical Society of America* **47**, 1440–1447.

Teja A.S. and Rice P. 1981a. Generalized corresponding states method for viscosities of liquid mixtures. *Industrial and Engineering Chemistry: Fundamentals* **20**, 77–81.

Teja A.S. and Rice P. 1981b. The measurement and prediction of the viscosities of some binary liquid mixtures containing n-hexane. *Chemical Engineering Science* **36**, 7–10.

Van Genuchten M.T. 1978. *Calculating the unsaturated hydraulic conductivity with a closed form analytical model*. Report 78-WR-08, Princeton University, NJ.

White J.E. 1975. Computed seismic speeds and attenuation in rocks with partial gas saturation. *Geophysics* **40**, 224–232.

Worthington P.F. 1991. Reservoir characterization at the mesoscopic scale. In: *Reservoir Characterization II* (eds L.W. Lake *et al.*), pp.123–165. Academic Press, Inc.

Yin C.S., Batzle M.L. and Smith B.J. 1992. Effects of partial liquid/gas saturation on extensional wave attenuation in Berea sandstone. *Geophysical Research Letters* **19**, 1399–1402.

Zimmerman R.W. 1991. *Compressibility of Sandstones*. Elsevier Science Publishing Co.